Selective Trapping of Labile S$_3$ in a Porous Coordination Network and the Direct X-ray Observation

Hiroyoshi Ohtsu,[†] Wanuk Choi,[†] Nazrul Islam,[†] Yoshitaka Matsushita,[‡] and Masaki Kawano*,[†]

[†]The Division of Advanced Materials Science, Pohang University of Science and Technology (POSTECH), San 31, Hyoja-dong, Pohang 790-784, Korea

[‡]NIMS Beamline Station at SPring-8 (BL15XU), National Institute for Materials Science (NIMS), Kouto 1-1-1, Sayo-cho, Hyogo 679-5148, Japan

S *Supporting Information*

ABSTRACT: S$_3$ is one of the basic allotropes of sulfur but is still a mysterious labile species. We selectively trapped S$_3$ in a pore of a thermally stable coordination network and determined S$_3$ structure by *ab initio* X-ray powder diffraction analysis. S$_3$ in a pore has a C$_{2v}$ bent structure. The network containing trapped S$_3$ is remarkably stable under ambient conditions and is inert to photoirradiation. S$_3$ in the network could be transformed to S$_6$ by mechanical grinding or heating in the presence of NH$_4$X (X = Cl or Br). S$_6$ could be reverse-transformed to S$_3$ by photoirradiation. We also determined the structure of the network containing S$_6$ by *ab initio* X-ray powder diffraction analysis.

Sulfur has various allotropes, including small ones (S$_n$, $n < 6$) that cannot be isolated from the mixture of small allotropes in a gas phase or in a solid Ar matrix.[1−4] These small allotropes are reactive and readily initiate successive reactions.[4−7] Quantum calculation has been used to calculate the structures of small sulfur allotropes,[8−11] but no one has reported their clear structural evidence and chemical properties except for estimation by rotational spectroscopy of S$_3$[12] and S$_4$.[12,13] Here we report selective encapsulation of S$_3$ in a crystalline porous coordination network, determination of the structure of S$_3$ by *ab initio* X-ray powder diffraction (XRPD) analysis, and the chemical properties of S$_3$. S$_3$ was significantly stabilized in this network. We also noticed reversible molecular transformation of S$_3$ to S$_6$ induced by mechanical grinding or heating with NH$_4$X (X = Cl or Br), the reverse transformation of S$_6$ to S$_3$ by photoirradiation, and polymerization of sulfur in a pore. Usually, trisulfur has been found as a stable anion radical, S$_3^−$, in zeolite, as in the pigment "Ultramarine".[14−18] However, in this study we succeeded in trapping and observing a small neutral sulfur allotrope that is quite unstable under ambient conditions.

To encapsulate small reactive sulfur allotropes, we chose a network, [ZnI$_2$(TPT)$_3$]$_n$, (network **1**, TPT = 2,4,6-tris(4-pyridyl)triazine) which has permanent porosity and robustness.[19,20] These features can be used for many applications, e.g. as a crystalline molecular flask in which unstable species can be encapsulated and analyzed by crystallography.[21−25] Network **1** can be readily obtained by heating an interpenetrated network,[26] which can be obtained as a powder by instant

mixing of ZnI$_2$ and TPT in nitrobenzene and methanol.[27] Network **1** has a saddle-type structure with a pore size, ~6.2 Å × 8.5 Å, and pore dimensions, ~8.3 Å × 10.5 Å. It is thermally stable enough to maintain porosity until 673 K; its pores can reversibly encapsulate small molecules, such as nitrobenzene or iodine, and are of appropriate size to encapsulate sulfur allotropes smaller than S$_8$.

In this work, we trapped a small sulfur allotrope in a pore of network **1** by sulfur vapor diffusion at 533 K for 6 h under vacuum (initial vacuum rate, ~70 Pa; 0.095 mmol of network **1** and 2.8 mmol of S$_8$ in a 14-mL vessel: Supporting Information [SI]). After exposure to sulfur vapor, network **1** powder changed from pale yellow to bright yellow, and the XRPD pattern clearly changed (Figure 1a,b). The changes of the peak
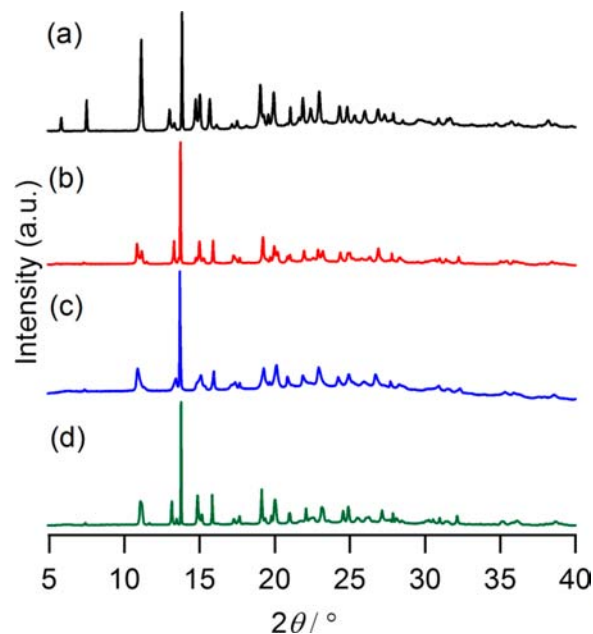
Figure 1. Change in XRPD pattern of [ZnI$_2$(TPT)$_3$]$_n$ powder after sulfur encapsulation. (a) Original network **1**, (b) network **2** with encapsulated sulfur, (c) network **3** with encapsulated sulfur, and (d) network **4** with encapsulated polymeric sulfur 2θ is unified with λ = 1.54056 Å.

and relative peak intensity suggest that sulfur was included in pores of the network. After encapsulating sulfur, the crystal system of network **1** changed from $a = 30.360$ Å, $b = 12.775$ Å, $c = 13.5826$ Å, *Pccn* to $a = 30.690$ Å, $b = 6.595$ Å, $c = 12.824$ Å, $\beta = 91.558°$, *Pn*. The structure of the sulfur-encapsulating network, i.e., network **2**, was solved by *ab initio* XRPD analysis (SI). We also observed two other sulfur-encapsulating networks: network **3** (Figure 1c) and network **4** (Figure 1d); these will be discussed later. The structure of network **2** was first solved by using the model of the original network **1** and several combinations of individual sulfur atoms to obtain the initial structural information about sulfur allotropes (using DASH[28]). All solutions showed an S_3 moiety in a pore of the porous coordination network. Using an S_3 model obtained by a rotational spectroscopic experiment,[12] *ab initio* XRPD analysis was performed again. With the use of the S_3-encapsulating model, the structure was refined with soft restraints for geometrical parameters by the Rietveld method (refined with the programs RIEAN-FP[29] and VESTA;[30] details are in SI). The good agreement between experimental and calculated diffraction patterns shows the correctness of the structure (Figure 2a). X-ray and elemental analyses suggest that S_3 is
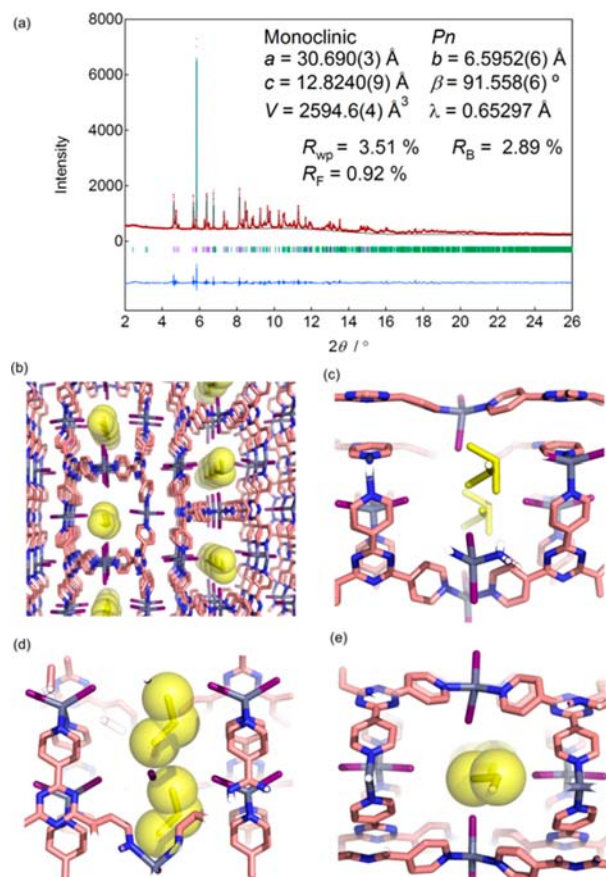
Figure 2. (a) Experimental (red), calculated (black), and difference (blue) XRPD profiles from the final Rietveld refinement of network **2**. The experimental pattern was obtained at BL15XU in SPring-8. (b) View with a major component of S_3 along *b*-axis (occupancy factor = 0.623). C, pink; N, blue; Zn, gray; I, purple; S, yellow. (c) Magnified view showing disordered S_3 molecules (occupancy factor = 0.623 and 0.377). (d) View with a major component of S_3 along *c*-axis (occupancy factor = 0.623). (e) View with a major component of S_3 along *b*-axis (occupancy factor = 0.623).

selectively trapped in a pore of network **1**. This is the first crystal structure determination of a reactive sulfur allotrope smaller than S_6. The open-triangle C_{2v} structure of S_3 is in good agreement with structures obtained using rotational spectroscopy.[8−13] The S_3 in a pore was disordered at two positions (Figure 2c). Notably, the short interatomic distances between sulfur and iodide in the major component of S_3 are 3.3 Å and 3.4 Å, each of which are considerably shorter than the sum (3.8 Å) of their van der Waals radii; this difference indicates a strong interaction between S_3 and iodide. Heating network **2** at 453 K regenerated network **1**. To confirm the unique presence of S_3 in network **2**, rather than a mixture of small sulfur allotropes like S_2, S_4, and S_5, we performed reflection FT-IR and reflection Raman microspectroscopic measurements of pure samples of each powder. The presence of S_3 was supported by the characteristic peak of S_3 in the vibrational spectra.[4] The S_3 trapped in network **2** produces a shoulder at ~680 cm^{-1} in the IR spectrum that corresponds to the S_3 asymmetric stretching mode (Figure S1). In addition, the absences of the characteristic Raman peak at 720 cm^{-1} for S_2 and of the IR peak at 650 cm^{-1} for S_4 support the X-ray powder analysis result (Figure S2; any experimental data of S_5 have not been reported). Usually in zeolite, S_3 exists as anions S_3^- and S_3^{2-}.[14−18] Therefore, we used spectroscopy to investigate whether these ions formed in network **2**. Results indicated that the S_3 in a pore exists as a neutral allotrope but not as S_3^- or S_3^{2-}:[14−18] we confirmed by the absence of IR peaks of S_3^{2-} (868, 487 cm^{-1}) the electron spin resonance (ESR) to be silent (unlike S_3^- radical anion) and the absence of UV−vis peaks of S_3^- at 595 nm.

Diffuse reflectance UV−vis spectra also provided the evidence of existence of S_3 in a pore. In normalized difference spectra of networks **1** and **2** (Figure S3B), network **2** has an additional absorption band at ~420 nm, which is attributable to S_3.[2,3] From X-ray analysis and spectroscopic results, we confirmed that only S_3 was selectively trapped in the pore of network **2** even though gaseous sulfur contains many sulfur allotropes (S_2 to S_8), of which S_3 has been estimated to contribute <0.1% at 573 K in saturated sulfur vapor.[2]

The S_3 trapped in network **2** is remarkably stable: the XRPD pattern did not change over 2−3 months even though the powder of network **2** was left in ambient conditions. Thermogravimetry/differential scanning calorimetry (TG/DSC) of network **2** showed a weight decrease at temperatures >500 K, which indicates that S_3 evaporated from the pores of the network (Figure S4).

Usually, sulfur allotropes are quite sensitive to photoirradiation. Therefore, we tested whether UV−vis light irradiation affects S_3 powder. Photoirradiation with a xenon lamp at 300−473 K produced no change in the XRPD pattern (Figure S5).

This result suggests that S_3 is unaffected by photoirradiation when encapsulated in a pore, unlike free sulfur allotropes.[1] Because ozone is reasonably stable in the absence of reactants at ambient conditions, it is not surprising that ozone analogue S_3 in itself can be stable and inert in an isolated state.

On rare occasions, when we exposed network **1** powder to sulfur vapor, we obtained another phase (network **3**) that shows an XRPD pattern (Figure 1c) different from that of network **2**. The structure of network **3** was also solved by *ab initio* XRPD analysis. Network **3** encapsulates S_6 in its pore. The good agreement between the experimental and calculated diffraction patterns in the Rietveld refinement confirms the

correctness of the structure (Figure 3a). The refinement of the structure converged with the site occupancy of 0.5 for each
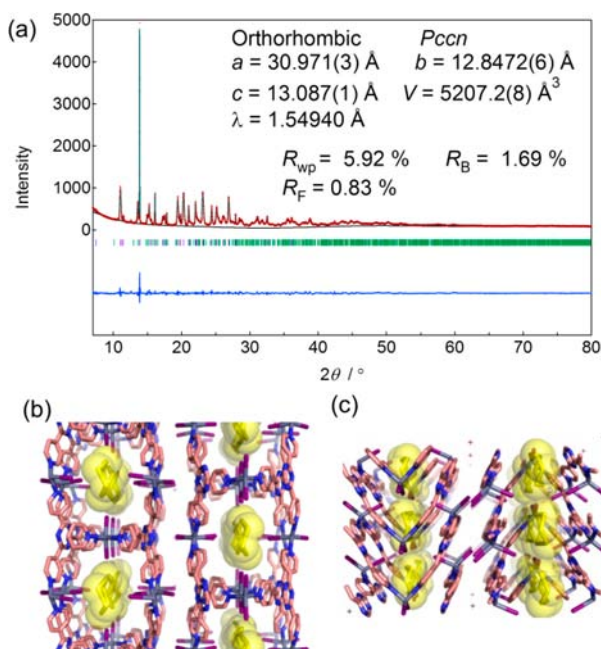
Figure 3. (a) Experimental (red), calculated (black), and difference (blue) XRPD profiles from the final Rietveld refinement of network **2**. The experimental pattern was obtained at BL9B in PAL. (b) View along *c*-axis. Occupancy factor of S_6 = 0.5. (c) View along *b*-axis. Color codes are as in Figure 2.

sulfur atom. These results show that 0.5 S_6 molecules exist in each pore; this result corresponds with elemental analysis data. The S_6 in a pore forms a six-membered ring with a chair conformation that is typical for a discrete S_6 molecule.[1] The interatomic distances between sulfur and iodide (3.1 Å and 3.4 Å) are shorter than the sum (3.8 Å) of their van der Waals radii. Like S_3, this difference indicates a strong interaction between S_6 and iodide. S_6 itself cannot enter the pore physically because the pore opening is smaller than S_6.

Indeed, an attempt to encapsulate S_6 into a pore using a CH_2Cl_2 solution of S_6 was unsuccessful. Therefore, the only way to encapsulate S_6 is by synthesizing it from smaller sulfur molecules after they enter the pores. However, S_3 in network **2** was never converted to S_6 by heating. Because we obtained network **3** just a few times, we suspected that the S_6 formation in network **1** was induced by some impurity in the starting materials. TPT sometime contains NH_4Cl as an impurity. Indeed, elementary analysis suggests the formation of (network **1**)·$(S_6)_{0.5}$·$(NH_4Cl)_{0.25}$ indicates inclusion of NH_4Cl in the pore. Therefore, we tried using NH_4Cl to convert S_3 to S_6 in a pore of network **2**.

When network **2** was heated at 473 K with NH_4Cl for 6 h under vacuum (~70 Pa, 0.060 mmol of network **2** and 0.063 mmol of NH_4Cl in a 4-mL vessel), the XRPD pattern changed to that of the network that traps S_6 (Figure 4). Because the transformation of $2S_3$ to S_6 did not occur in the absence of NH_4Cl, it may catalyze the S_6 ring formation. This transformation reaction also occurred when network **2** was heated with NH_4Br at 573 K *in vacuo* (Figure S6), suggesting that an ammonium cation triggered the transformation as a proton donor[31] (Scheme 1). To confirm this mechanism, network **2** was exposed successively to dry HCl and NH_3. When network
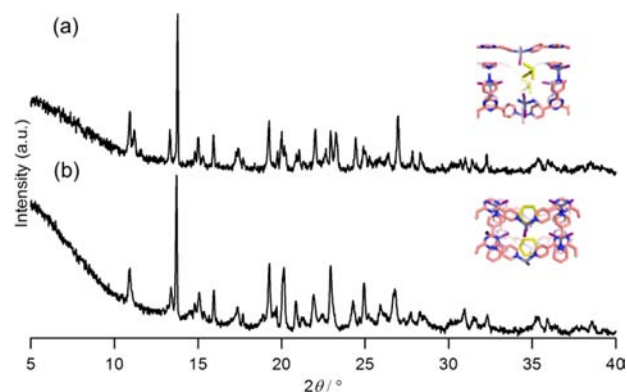
Figure 4. Powder pattern changes by heating with NH_4Cl and corresponding structures. (Insets) (a) S_3 encapsulating network **2**; (b) after heating with NH_4Cl. The powder pattern of (b) corresponds to that of network **3**.

Scheme 1. Possible Mechanism of Ring Formation
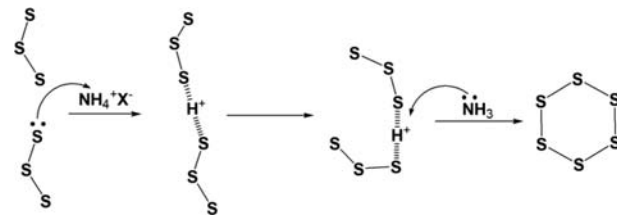
2 was exposed to dry HCl, the XRPD pattern drastically changed. After subsequent exposure of this network to NH_3, the XRPD pattern of the powder changed to that of network **3** (Figure S7).

As a control, network **2** was exposed first to NH_3 and then to dry HCl; in this case, NH_3 did not induce drastic diffraction pattern changes compared with HCl. After introduction of dry HCl the diffraction pattern became similar to that of network **3** (Figure S8). Therefore, we conclude that transformation of $2S_3$ to S_6 in the presence of NH_4Cl is triggered by a proton from an ammonium cation (Scheme 1). Furthermore, the reverse transformation of S_6 to $2S_3$ was observed after 365-nm excitation of network **3** at 300 K for 5 h (Figure S9); this indicates that, in the pore, S_3 is more stable to light irradiation than is S_6.

Bright-yellow powder of network **2** can be converted to pale-yellow powder of network **3** by mechanical grinding at room temperature (Figure S10), even though heating S_3 never changed it to S_6 in a pore. Basically, S_6 is more stable than S_3; therefore, S_3 conversion to S_6 is an enthalpically favorable reaction. Because at high temperature this conversion reaction can be entropically not desirable, this conversion did not occur.

We examined the possibility of sulfur polymerization in a pore. Below 573 K, no polymerization was observed in network **1**. However, when sulfur encapsulation was performed in a sealed tube at 653 K *in vacuo*, a brownish powder (network **4**) was obtained which showed an XRPD diffraction pattern different from those of networks **1**, **2**, and **3** (Figure 1d). The diffuse-reflectance UV−vis spectrum of network **4** showed broad absorption bands reaching 1450 nm, i.e., the near-IR region (Figure S11). The IR spectrum showed a weak band at 692 cm^{-1} which may correspond to an asymmetric stretching band of the terminal S−S bond (Figure S12). In addition, ESR of the network **4** powder showed a signal with g = 2.004

11451

dx.doi.org/10.1021/ja4046718 | *J. Am. Chem. Soc.* 2013, 135, 11449−11452

(Figure S13), which corresponds to that of one-dimensional polymerized sulfur.[32,33] These observations indicate that polymerized sulfur was generated in the pores at 653 K. TG measurement of network **4** showed weight loss of ~5.0% at 573 K, which indicates that sulfur escaped from the pore at temperatures less than the decomposition temperature (673 K) of the network (Figure S14). Because polymerized sulfur allotropes are usually not stable and are readily transformed to S_8 or other ring compounds,[1] the S−S bond in the polymer dissociates at high temperatures. Although we could determine the network framework of network **4** by *ab initio* powder X-ray analysis, we could not determine reasonable models for the polymerized sulfur, very likely due to severe disorder and the small amount of sulfur. Because the amount of encapsulated sulfur is small (5.2% in $[(ZnI_2)_3(TPT)_2(S)_{2.72}]$), the poly-merized sulfur is randomly distributed among pores and has smaller occupancy factors than do S_3 and S_6.

Our findings about S_3 provide insight into the labile nature of sulfur allotropes. Considering the small amount of S_3 in sulfur vapor at high temperatures, we can assume that the selective formation of S_3 and polymerized sulfur in a pore were induced by more reactive and more abundant sulfur species like S_2 (which is a major species in high-temperature sulfur vapor) trapped in the pores. This encapsulation approach using a crystalline porous material combined with analyses not only of single crystals but also *ab initio* powder structure analysis with synchrotron light can be applied to explore new chemistry, especially of unstable species, to improve understanding of molecular structure, chemical nature, and reaction mechanisms.

ASSOCIATED CONTENT

Ⓢ Supporting Information

Experimental details, elemental analysis, *ab initio* XRPD analysis, Raman spectra, IR spectra, UV−vis−NIR spectra, ESR spectra, XRPD patterns, and TG-DSC results, and crystallographic details (CIF). See CCDC entries 919862 and 919863; these data can be downloaded free of charge via www.ccdc.cam.ac.uk/conts/retrieving.html (or obtained from the Cambridge Crystallographic Data Centre, 12 Union Road, Cambridge CB21EZ, UK; fax (+44) 1223033; or deposit@ccdc.cam.ac.uk). This material is available free of charge via the Internet at http://pubs.acs.org.

AUTHOR INFORMATION

Corresponding Author
mkawano@postech.ac.kr

Notes
The authors declare no competing financial interest.

ACKNOWLEDGMENTS

REFERENCES

(1) Steudel, R.; Eckert, B. *Top. Curr. Chem.* **2003**, *230*, 1.
(2) Steudel, R.; Steudel, Y.; Wong, M. W. *Top. Curr. Chem.* **2003**, *230*, 117.
(3) Meyer, B. *Chem. Rev.* **1976**, *76*, 367.
(4) Eckert, B.; Stuedel, R. *Top. Curr. Chem.* **2003**, *231*, 31.
(5) Nakayama, J.; Aoki, S.; Takayama, J.; Sakamoto, A.; Sugihara, Y.; Ishii, A. *J. Am. Chem. Soc.* **2004**, *126*, 9085.
(6) Steliou, K.; Gareau, Y.; Harpp, D. N. *J. Am. Chem. Soc.* **1984**, *106*, 799.
(7) Steliou, K.; Gareau, Y.; Milot, G.; Salama, P. *J. Am. Chem. Soc.* **1990**, *112*, 7819.
(8) Wong, M. W. *Top. Curr. Chem.* **2003**, *231*, 1.
(9) Murray, C. W.; Handy, N. C.; Amos, R. D. *J. Chem. Phys.* **1993**, *98*, 7145.
(10) Rice, J. E.; Amos, R. D.; Handy, N. C.; Lee, T. J.; Schaefer, H. F. *J. Chem. Phys.* **1986**, *85*, 963.
(11) Millefiori, S.; Alparone, A. *J. Phys. Chem. A* **2001**, *105*, 9489.
(12) McCarthy, M. C.; Thorwirth, S.; Gottlieb, C. A.; Thaddeus, P. *J. Am. Chem. Soc.* **2004**, *126*, 4096.
(13) Thorwirth, S.; McCarthy, M. C.; Gottlieb, C. A.; Thaddeus, P.; Gupta, H.; Stanton, J. F. *J. Chem. Phys.* **2005**, *123*, 054326.
(14) Seel, F. *Stud. Inorg. Chem.* **1984**, *5*, 67.
(15) Hoffmann, S. K.; Goslar, J.; Lijewski, S.; Olejniczak, I.; Jankowska, A.; Zeidler, S.; Koperska, N.; Kowalak, S. *Microporous Mesoporous Mater.* **2012**, *151*, 70.
(16) Reinen, D.; Linder, G. *Chem. Soc. Rev.* **1999**, *28*, 75.
(17) Tarling, S. E.; Barnes, P.; Kilnowski, J. *Acta Crystallogr.* **1988**, *B44*, 128.
(18) Kowalak, S.; Jankowska, A.; Zeidler, S.; Wieckowski, A. B. *J. Solid. State. Chem.* **2007**, *180*, 1119.
(19) Martí-Rujas, J.; Islam, N.; Hashizume, D.; Izumi, F.; Fujita, M.; Kawano, M. *J. Am. Chem. Soc.* **2011**, *133*, 5853.
(20) Ohara, K.; Martí-Rujas, J.; Haneda, T.; Kawano, M.; Hashizume, D.; Izum, F.; Fujita, M. *J. Am. Chem. Soc.* **2009**, *131*, 3860.
(21) Kawamichi, T.; Haneda, T.; Kawano, M.; Fujita, M. *Nature* **2009**, *461*, 633.
(22) Kawamichi, T.; Inokuma, Y.; Kawano, M.; Fujita, M. *Angew. Chem. Int. Ed.* **2010**, *49*, 2375.
(23) Inokuma, Y.; Kawano, M.; Fujita, M. *Nat. Chem.* **2011**, *3*, 349.
(24) Haneda, T.; Kawano, M.; Kawamichi, T.; Fujita, M. *J. Am. Chem. Soc.* **2008**, *130*, 1578.
(25) Kawamichi, T.; Kodama, T.; Kawano, M.; Fujita, M. *Angew. Chem., Int. Ed.* **2008**, *47*, 8030.
(26) Biradha, K.; Fujita, M. *Angew. Chem., Int. Ed.* **2002**, *41*, 3392.
(27) Kawano, M.; Haneda, T.; Hashizume, D.; Izumi, F.; Fujita, M. *Angew. Chem., Int. Ed.* **2008**, *47*, 1269.
(28) David, W. I. F.; Shankland, K.; van de Streek, J.; Pidcock, E.; Motherwell, W. D. S.; Cole, J. C. *J. Appl. Crystallogr.* **2006**, *39*, 910.
(29) Izumi, F.; Momma, K. *Solid State Phenom.* **2007**, *130*, 15.
(30) Momma, K.; Izumi, F. *J. Appl. Crystallogr.* **2001**, 653.
(31) Maleki, B.; Salehabadi, H. *Eur. J. Chem.* **2010**, *4*, 377.
(32) Gardner, D. M.; Fraenkel, G. K. *J. Am. Chem. Soc.* **1956**, *78*, 3279.
(33) Kozhevnikov, V. F.; Payne, W. B.; Olson, J. K.; McDonald, C. L.; Inglefield, C. E. *J. Chem. Phys.* **2004**, *121*, 7379.